A Large-Scale Multimodal CMOS Biosensor Array with 131,072 Pixels and Code Division Multiplexed Readout

Kangping Hu, Christopher E. Arcadia, and Jacob K. Rosenstein
School of Engineering
Brown University, Providence, RI 02912, USA

***Abstract*— This paper presents a large-scale fully integrated multimodal sensor array for biological imaging. The 512×256 sensor array can perform spatially-resolved electrochemical impedance spectroscopy (EIS) with switching frequencies up to 100 MHz, acquire multi-color optical images, and sense pH using titanium nitride (TiN) ion sensitive field effect transistors (ISFETs). The chip features code-division multiplexed (CDM) readout of groups of pixels simultaneously, enabling extended integration times at a given frame rate. The system is implemented in 180 nm CMOS with 9.5 μm × 11.5 μm pixels. Its overall fill factor is 57%, including peripheral control and readout circuits, yielding a wide-field spatially-resolved multimodal biosensing platform for advanced cell culture applications.**

Keywords*— *biosensor, impedance spectroscopy, electrochemical, ISFET, image sensor, CMOS, dielectric spectroscopy, array, cell culture

I. Introduction

Integrated circuits continue to gain traction in a diverse array of biomedical applications, including neural recording systems, DNA sequencing instruments, and smart cell culture platforms which demand creative solutions for dense multimodal sensor integration [1]–[6].

There are several types of CMOS-compatible sensors that can provide useful measurements of growing cell cultures. The most classical options are photodiode arrays, which can be used for optical imaging of cells' shapes and positions even without lenses [1], [7], [8], although lens-free contact imaging often does not reach the diffraction limit. Cellular metabolism can be monitored indirectly through pH changes, recorded by ion-sensitive field-effect transistors (ISFETs) [9]. Electrochemical impedance spectroscopy (EIS) can provide spatially-resolved images of the local conductivity and dielectric constant, which relate to properties of cell membranes, proteins, and extracellular matrix. EIS measurements are also frequency-dependent, offering another dimension of information [1], [2], [4], [7], [10]. Recognizing the diversity and multi-scale nature of cellular processes, a multimodal lens-free CMOS sensor array with a sufficiently large active sensing area could enable wide-field monitoring of cells, colonies, or even whole tissues at a fraction of the size and cost of traditional microscopes.

This work was supported in part by a grant from the Defense Advanced Research Projects Agency (DARPA), and by the National Science Foundation under Grant No. 2027108. The authors thank Tianyi Shen and Domenico Pacifici for help with optical measurements.

Here, we present a multimodal CMOS sensor array that measures radio-frequency impedance spectra, pH, and visible light, across 131,072 pixels. Intended for long-term cell culture monitoring, this design prioritizes a large uninterrupted sensing area. It achieves a 57% fill factor, with the active sensing region occupying more than half of the chip surface. With thousands of co-located EIS, pH, and optical measurements, this system can capture detailed spatially-resolved recordings of cellular growth and metabolism.

II. CMOS Sensor Array Design

A. Pixel Design

The active sensing area has 131,072 pixels arranged in a 512×256 array (Fig. 1). Each pixel contains an exposed surface electrode, a high-frequency impedance measurement circuit, an NMOS ISFET for pH sensing, and three photodiodes for color-sensitive optical imaging. The current is steered between two shared column outputs using another set of control signals (θ and $\bar{\theta}$). Depending on how θ is configured, the readout can support either time-division multiplexing (TDM) or code-division multiplexing (CDM). Only one type of sensor is active at a time for minimal crosstalk between sensing modes, and inactive pixels can optionally be routed to a dummy column to reduce pixel-to-pixel parasitic coupling. The details of each measurement mode are explained in the following subsections.

1) EIS Measurement: The EIS circuits support impedance measurements up to 100 MHz using a switched capacitor circuit with non-overlapping clocks (Φ_1 and Φ_2) to rapidly charge and discharge the electrode. In comparison to traditional kHz EIS, radio frequency operation reduces Debye screening, producing measurements sensitive to the dielectric environment farther from the electrode surface [4].

2) Color-sensitive Optical Imaging: To support ratiometric absorption measurements of cell optical density across multiple wavelengths, each pixel contains a photodetector in which three diodes share the same P-substrate, but have isolated N-well cathode contacts which are biased to V_0, V_1, and V_2. The photodiodes are surrounded by guard rings for improved isolation. A cross-section view of the pixel is shown in Fig. 3(b). Depending on the bias voltages, the electric field distribution will cause the cathodes to collect photons absorbed at different depths in the P-substrate. By separately collecting currents from each cathode contact, the sensor can achieve tunable wavelength selectivity [11].

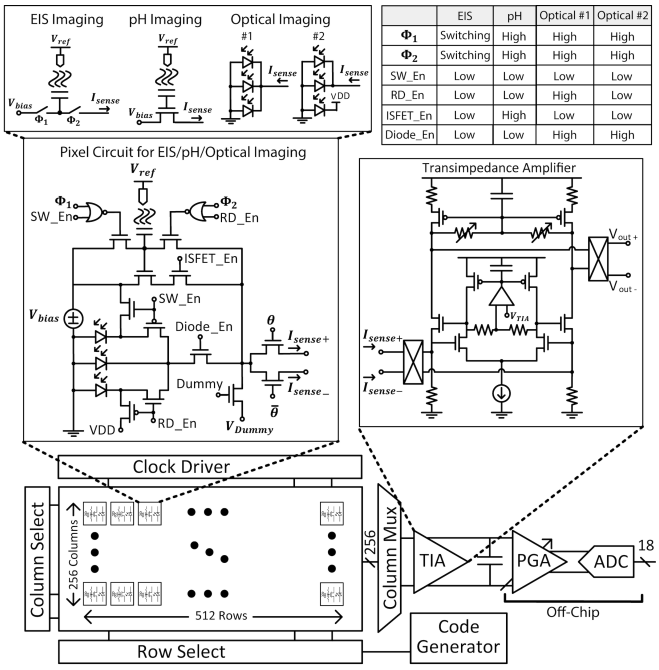

	EIS	pH	Optical #1	Optical #2
Φ_1	Switching	High	High	High
Φ_2	Switching	High	High	High
SW_En	Low	Low	Low	Low
RD_En	Low	Low	High	Low
ISFET_En	Low	High	Low	Low
Diode_En	Low	Low	High	High

Fig. 1. Simplified circuit diagram of the 512 x 256 pixel biosensor array. Each pixel can be configured to measure electrochemical impedance, pH, or visible light.

Although there is a sensitivity penalty, this arrangement allows us to assemble a color image from multiple exposures, without a color filter mosaic. The photodiodes have a minimal impact on the total sensor area, because they are positioned underneath the required spacing between the top metal electrodes.

3) pH Sensing: An ISFET is a transistor whose floating gate is connected to an electrode exposed to an ionic solution, and which measures pH through the relationship between the gate's surface charge and the device's threshold voltage. The pH measurement is performed with both EIS switches disabled, but these switches can optionally also be used to reset trapped charges and reduce ISFET drift [12].

Demonstrations of ISFETs in standard CMOS often use Si_3N_4 as the gate passivation layer or deposit additional pH sensitive dielectric materials. Here, instead of depositing additional layers, we use a single post-processing step to chemically etch away the aluminum top metal, exposing the electrodes' underlying titanium nitride (TiN) diffusion barrier, which is a conductive and highly stable material that can be used for both pH and impedance sensing [13].

B. Column Amplifiers

Column outputs from the array are directed into a high-bandwidth differential current buffer (Fig. 1). The output voltage is low-pass filtered, amplified, and then digitized by an external 18-bit ADC at 500 kS/s. The current buffers are gain-boosted common gate amplifiers with a simulated bandwidth of 200 MHz and are used to maintain a low input impedance as well as to clamp the input voltage. Differential chopping is used to suppress 1/f noise and offsets.

All of the columns are multiplexed onto a single readout channel, which simplifies calibration and reduces the chip area and design complexity at the cost of lower frame rates. This tradeoff is acceptable since recording cell culture growth typically involves time-lapse imaging over the course of hours or days.

C. Code Division Readout

The addressing logic supports either time-division (TDM) or code-division multiplexed (CDM) readout (Fig. 2). In TDM, pixels are measured one at a time. In contrast, CDM enables concurrent readout from blocks of pixels to extend the integration times for a given frame rate and improve the common-mode shielding from neighboring pixels [14].

We previously implemented an EIS array with 64-bit CDM readout [14], and here we further expand the hardware capabilities to support up to 256-bit codes. A set of orthogonal codes is generated by on-chip logic (Fig. 2c), and each code is assigned to a row. The modulated currents from each row are summed into the same column, and after the signals are digitized, the time series of each column is multiplied by the encoding matrix to decode the data for each row.

All codes have a constant sum of $\sqrt{\text{code length}}$, which helps to reduce distortion, but which adds a DC offset to the output current that can saturate the column amplifier. In consideration of each sensor's different typical current range, we often use 256-bit CDM for optical imaging, 64-bit CDM for EIS, and TDM for pH sensing.

With a 3 kHz code clock, EIS and optical images are each acquired in ≈ 50 seconds. For pH sensing, we allocate 1 ms/address, or ≈ 2.5 minutes per full frame. During time-lapse cell culture recordings, the system can record a set of full-frame EIS, pH, and optical images every 5 minutes.

III. Measurement Results

A. Layout and Packaging

The circuit is implemented in a 180 nm 1P6M CMOS process, with 9.5 μm $\times$ 11.5 μm pixel size and an active sensing area occupying 14.3 mm^2 of the 25 mm^2 chip (Fig. 3(c)(d)). The chip is wirebonded to a small printed

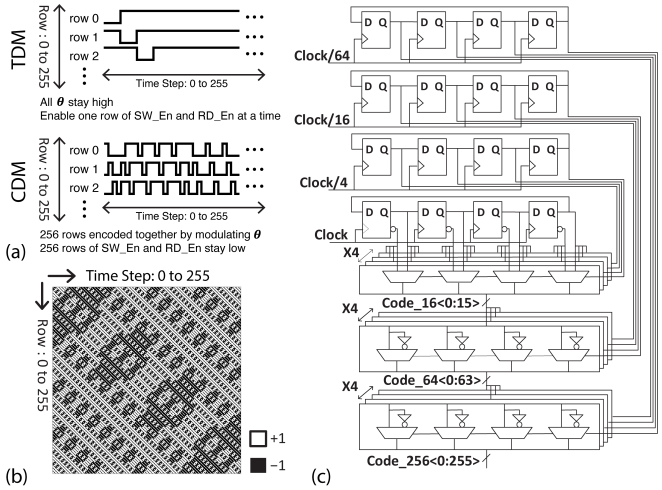

Fig. 2. (a) Timing diagram comparison between time-division and 256-bit code-division readout. (b) The binary matrix of 256-bit orthogonal codes. (c) On-chip logic generates sets of orthogonal codes up to 256 bits.

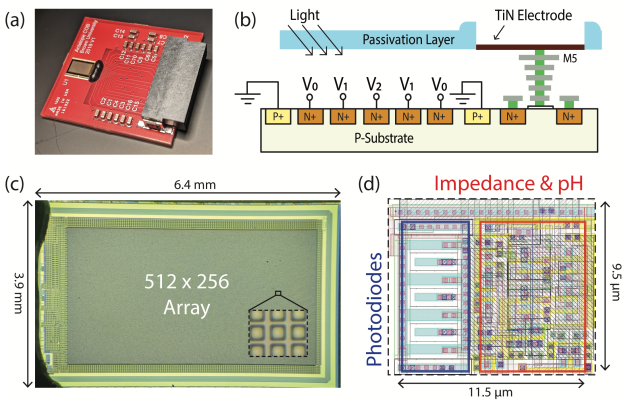

Fig. 3. (a) The chip is fabricated in 180 nm CMOS, and wirebonded to a small chip-on-board module. (b) Cross-section of a pixel. (c) The die is 3.9×6.4 mm^2. (d) Each multi-modal pixel occupies 11.5×9.5 μm^2.

circuit board, which is connected to a custom data acquisition board with an external ADC. The bondwires are encapsulated with epoxy (Fig. 3(a)), and a plastic fluid chamber is mounted around the chip with silicone adhesive.

B. EIS Sensitivity

The sensing array contains an extra column with a series of built-in capacitors for self-testing (Fig. 4(c)). This test column uses two metal layers to create a varying capacitance, which increments by 8 aF, and repeats every 64 rows. We measured this test column with a 100 MHz switching frequency, a differential bias voltage of 400 mV, 110 dBΩ transimpedance gain, 64-bit codes with a 3 kHz code clock, and differential chopping at 100 kHz to suppress the 1/f noise (Fig. 4(a)). Taking repeated measurements from a single test pixel at 1 millisecond intervals, we observe an effective noise floor of 0.7 aF$_{rms}$ (7×10^{-19} Farads, Fig. 4(b)).

C. Photodiode Characterization

We collected measurements of the photodiode using 256-bit CDM while sweeping the excitation wavelength of a calibrated laser source (Fig. 4(d)). When the amplifier collects signals from all three cathodes (inset, left) (V_0, V_1, and V_2 in Fig. 3(b)), the response resembles a typical silicon photodiode, favoring red light. However, when we connect V_0 to V_{DD} (inset, right), the signal collected by the remaining cathodes V_1 and V_2 has a bandpass response with a maximum in the green band. The estimated peak responsivities are 195 mA/W (≈700nm) and 11 mA/W (≈525nm), corresponding to maximum quantum efficiencies of 35% and 2.7%.

D. pH Sensitivity

Fig. 4 (e) shows the response of the TiN ISFETs, measured in 0.1M potassium phosphate buffer with an Ag/AgCl reference electrode. To produce I-V curves for one ISFET pixel, we set V$_s$ = 0V, V$_d$ = 600 mV, and sweep V$_{ref}$. With V$_{gs}$ = 1.2 V, the sensitivity is 27.7 mV/pH. Fig. 4(f) shows the ISFET response to changes in solution pH.

E. Widefield Impedance Imaging

As an initial demonstration of the chip's ability to detect cellular-scale objects, we measured a dispersion of aluminum oxide particles (collected from sandpaper) suspended in

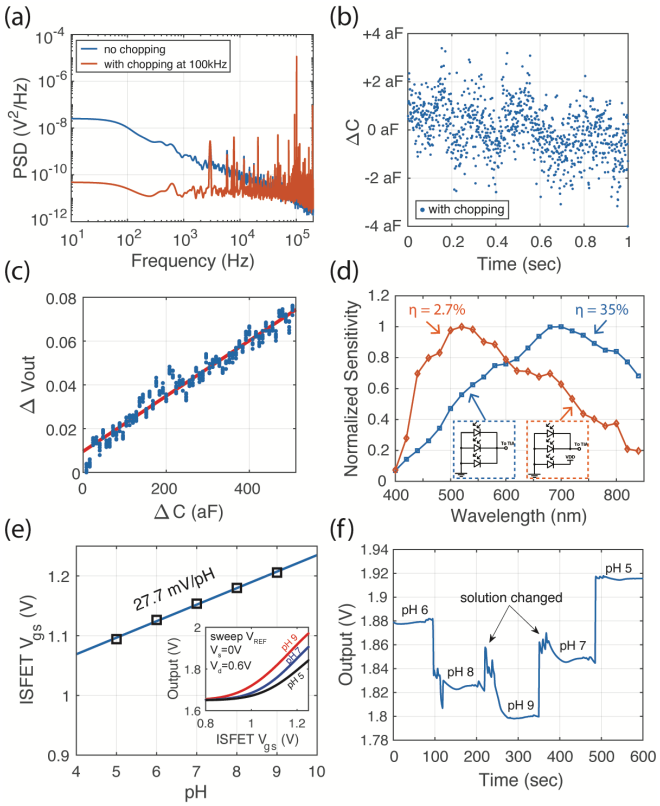

Fig. 4. Performance characterization of the multimodal CMOS biosensor array. (a) Measured power spectral density of the shared column amplifier, with and without chopping enabled. (b) At 1 ms acquisition intervals and 100 MHz switching, the electrochemical impedance noise floor corresponds to 0.7 attofarads RMS (1 aF = 10^{-18} F.) (c) Impedance calibration using a self-test column with ≈ 8 aF capacitance steps. (d) Measured optical wavelength selectivity in two photodiode modes. (e) The measured sensitivity of the TiN ISFETs is 27.7 mV/pH. (f) Transient response of a TiN ISFET. Five buffer solutions (0.1M potassium phosphate) with varying pH were exchanged manually.

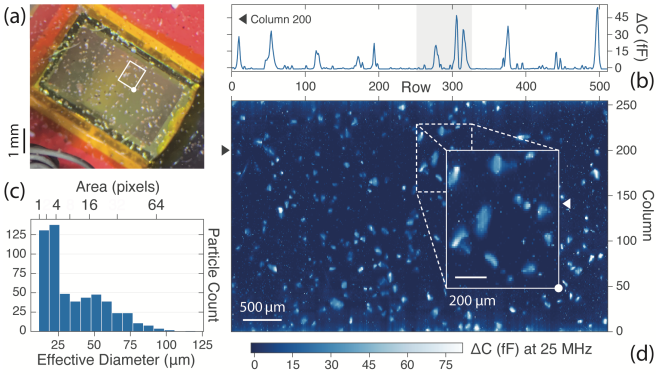

Fig. 5. (a) Photograph of sand particles on the sensor array, in buffer solution. (b) A cross-section of the measured impedance signal for column 200. (c) A histogram of effective diameters for the detected particles (562 total, 5.77% area coverage). (d) Impedance image of the sand particles shown in (a). Data were acquired at 25 MHz using 64-row code-division multiplexing in 0.1M potassium phosphate buffer.

potassium phosphate buffer. An Ag/AgCl reference electrode provided a constant potential bias to the solution.

Fig. 5 shows an EIS image where hundreds of sand particles are visible. The particles were mostly smaller than 100μm (Fig. 5(c)), with diverse shapes and geometrical features. The abundance of clearly detected particles (with a threshold of 5σ) near the one-pixel limit suggests that many

TABLE I

COMPARISONS WITH THE STATE OF THE ART

	This work	**[1]**	**[4]**	**[15]**	**[5]**
Modality	Impedance + pH + Optical	Impedance + Optical + Voltage + Stimulation	Impedance	Impedance + Voltage + Stimulation	pH + Optical
Array Size	131,072	21,952	65,536	59,760	4,096
Pixel Size	9.5×11.5 μm^2	16×16 μm^2	0.6×0.89 μm^2	13.5×13.5 μm^2	10×10 μm^2
Impedance Resolution	0.7 aF	-	0.5 - 1 aF	-	-
Max. Impedance Frequency	100 MHz	500 kHz	70 MHz	1 MHz	-
ISFET Material	TiN	-	-	-	Si_3N_4
ISFET Sensitivity	27.7 mV/pH	-	-	-	26.2 mV/pH
Multi-Color	Yes	No	-	-	No
Readout	CDM / TDM	TDM	TDM	TDM	TDM
Fill Factor (sensing area / chip area)	0.57	0.12	0.008	0.12	0.075
Technology	180 nm	130 nm	90 nm	180 nm	180 nm

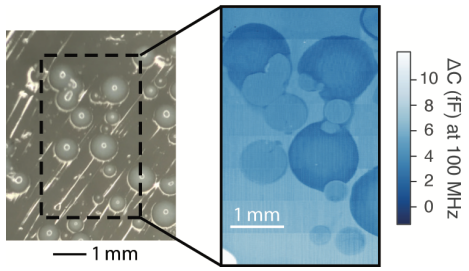

Fig. 6. A brightfield microscope image of live bacteria colonies (left), and a non-optical electrochemical impedance image of the same colonies, after being placed in contact with the sensor array (right). The capacitance image was acquired at 100 MHz using 64-row code-division multiplexing.

of the observed objects are smaller than $10\mu m$.

To illustrate the sensor's ability to image living bacteria cells, we cultured bacteria from a simple skin swab on lysogeny broth (LB) nutrient agar for 12 hours at 37°C. After incubation, the bacteria colonies (suspected to be *S. epidermidis*) were placed in contact with the sensor array. Fig. 6 shows an EIS image of the live colonies. The high contrast of this label-free non-optical image highlights the continued opportunities for low-cost and high performance integrated biosensor arrays.

F. Comparison with the state of the art

The comparisons in Table I show that this design has the largest array size and the highest fill factor in its class. It supports the highest EIS operating frequency and offers highly competitive detection limits. This work is also the first multimodal sensor array to include a CDM readout option and photodiodes with multi-color selectivity.

IV. CONCLUSION

We have presented a large-scale multimodal imaging array that can perform EIS, pH, and optical measurements. Future work will include applying this new platform to monitor the real-time growth of microbial colonies and integrating the multimodal sensor with appropriate fluidics and environmental control for advanced cell culture applications.

REFERENCES

[1] D. Jung, J. S. Park, G. V. Junek, S. I. Grijalva, S. R. Kumashi, A. Wang, S. Li, H. C. Cho, and H. Wang, "A 21952-Pixel Multi-Modal CMOS Cellular Sensor Array with 1568-Pixel Parallel Recording and 4-Point Impedance Sensing," *2019 Symposium on VLSI Circuits*, pp. C62–C63, 2019.

[2] B. P. Senevirathna, S. Lu, M. P. Dandin, J. Basile, E. Smela, and P. A. Abshire, "Real-time measurements of cell proliferation using a lab-on-cmos capacitance sensor array," *IEEE Transactions on Biomedical Circuits and Systems*, vol. 12, no. 3, pp. 510–520, June 2018.

[3] D. L. Bellin, H. Sakhtah, J. K. Rosenstein, P. M. Levine, J. Thimot, K. Emmett, L. E. P. Dietrich, and K. L. Shepard, "Integrated circuit-based electrochemical sensor for spatially resolved detection of redox-active metabolites in biofilms." *Nature communications*, vol. 5, p. 3256, jan 2014.

[4] F. Widdershoven, A. Cossettini, C. Laborde, A. Bandiziol, P. P. van Swinderen, S. G. Lemay, and L. Selmi, "A cmos pixelated nanocapacitor biosensor platform for high-frequency impedance spectroscopy and imaging," *IEEE Transactions on Biomedical Circuits and Systems*, vol. 12, no. 6, pp. 1369–1382, Dec 2018.

[5] X. Huang, H. Yu, X. Liu, Y. Jiang, M. Yan, and D. Wu, "A dual-mode large-arrayed cmos isfet sensor for accurate and high-throughput ph sensing in biomedical diagnosis," *IEEE Transactions on Biomedical Engineering*, vol. 62, no. 9, pp. 2224–2233, Sep. 2015.

[6] J. Abbott, T. Ye, K. Krenek, R. S. Gertner, S. Ban, Y. Kim, L. Qin, W. Wu, H. Park, and D. Ham, "A nanoelectrode array for obtaining intracellular recordings from thousands of connected neurons," *Nature Biomedical Engineering*, no. 2, pp. 232–241, 2020.

[7] T. Chi, J. S. Park, J. C. Butts, T. A. Hookway, A. Su, C. Zhu, M. P. Styczynski, T. C. McDevitt, and H. Wang, "A Multi-Modality CMOS Sensor Array for Cell-Based Assay and Drug Screening," *IEEE Transactions on Biomedical Circuits and Systems*, vol. 9, no. 6, pp. 801–814, 2015.

[8] H. Ji, P. Abshire, M. Urdaneta, and E. Smela, "CMOS contact imager for monitoring cultured cells," *2005 IEEE International Symposium on Circuits and Systems (ISCAS)*, pp. 3491–3494 Vol. 4, 2005.

[9] M. J. Milgrew and D. R. S. Cumming, "A Proton Camera Array Technology for Direct Extracellular Ion Imaging," *2008 IEEE International Symposium on Industrial Electronics*, pp. 2051–2055, 2008.

[10] G. Nabovati, E. Ghafar-Zadeh, A. Letourneau, and M. Sawan, "Smart Cell Culture Monitoring and Drug Test Platform Using CMOS Capacitive Sensor Array," *IEEE Transactions on Biomedical Engineering*, vol. 66, no. 4, pp. 1094–1104, 2018.

[11] A. Longoni, F. Zaraga, G. Langfelder, and L. Bombelli, "The transverse field detector (tfd): A novel color-sensitive cmos device," *IEEE Electron Device Letters*, vol. 29, no. 12, pp. 1306–1308, Dec 2008.

[12] N. Moser, C. L. Leong, Y. Hu, C. Cicatiello, S. Gowers, M. Boutelle, and P. Georgiou, "Complementary metal–oxide–semiconductor potentiometric field-effect transistor array platform using sensor learning for multi-ion imaging," *Analytical Chemistry*, vol. 92, no. 7, pp. 5276–5285, 2020.

[13] K. Hu, X. Lian, S. Dai, and J. K. Rosenstein, "Low noise cmos isfets using in-pixel chopping," in *2019 IEEE Biomedical Circuits and Systems Conference (BioCAS)*. IEEE, 2019, pp. 1–4.

[14] K. Hu, E. Kennedy, and J. K. Rosenstein, "High frequency dielectric spectroscopy array with code division multiplexing for biological imaging," in *2019 IEEE Biomedical Circuits and Systems Conference (BioCAS)*. IEEE, 2019, pp. 1–4.